Coercivity mechanism of anisotropic $Pr_2Fe_{14}B$ thin films with perpendicular texture

S. L. Chen, W. Liu, and Z. D. Zhang
Shenyang National Laboratory for Materials Science, Institute of Metal Research, and International Centre for Materials Physics, Chinese Academy of Sciences, 72 Wenhua Road, Shenyang, 110016, People's Republic of China
(Received 26 June 2005; revised manuscript received 14 October 2005; published 13 December 2005)

Anisotropic Pr-Fe-B thin films with perpendicular texture have been prepared by magnetron sputtering and subsequent heat treatment. After crystallization at 873 K, the films deposited at 773 K show a perpendicular anisotropic texture, due to the existence of a weak anisotropy in the as-deposited films. The deposition rate has been proved to be an important parameter for the control of microstructure, morphology, and coercivity. The coercivity mechanism of the anisotropic Pr-Fe-B films has been studied by analyzing the temperature dependence of coercivity from 5 to 300 K, based on the micromagnetic model. Nucleation of reversed domains, taking place preferentially at the grain surface where the magnetic anisotropy is reduced and the local demagnetization field is the highest, is determined to be the leading mechanism in controlling the magnetization reversal processes of the anisotropic Pr-Fe-B films. Though the grains in the films are strongly magnetically coupled, the magnetization reversal processes in the Pr-Fe-B thin films are not realized by uniform rotations of the magnetic moments.

DOI: 10.1103/PhysRevB.72.224419 PACS number(s): 75.70.Ak, 75.60.Jk, 75.70.Kw, 81.15.Cd

I. INTRODUCTION

Anisotropic $Nd_2Fe_{14}B$-based thin films have been widely investigated for their potential applications in micromagnetic devices, micromechanical devices, and magnetic-optical recording media.[1–4] Various methods of film depositions, such as magnetron sputtering,[5] molecular beam epitaxy,[6] as well as pulsed laser deposition,[4,7] have been used to prepare anisotropic $Nd_2Fe_{14}B$ films with *c*-axis texture. In order to achieve good permanent magnetic properties, one needs to reach a high coercivity and a reasonable remnant magnetization for the magnetic thin films. Therefore it is very important to understand in depth the coercivity mechanism of the permanent magnetic films.

The coercivity of the permanent magnets is usually dominated by the nucleation mechanism and/or the domain-wall pinning mechanism, depending sensitively on the microstructure and intrinsic magnetic properties of the magnets. It was reported that the coercivity of the sintered Nd-Fe-B magnets is controlled by different mechanisms in different temperature ranges,[8] and the coercivity mechanism of the isotropic Nd-Fe-B thin films is similar to that of the sintered Nd-Fe-B magnets.[9] It was reported also that, below 410 K, the magnetization process is dominated by the nucleation process for the isotropic Nd-Fe-B thin films.[9] However, the case is different for the anisotropic Nd-Fe-B thin films, in which the strong domain-wall pinning dominates the magnetization reversal processes in the temperature range from about 100 to 550 K.[9,10]

Compared to numerous studies on Nd-Fe-B thin films (as reviewed by Kruusing[11]), few studies have been focused on anisotropic Pr-Fe-B thin films.[12,13] The coercivity mechanism of the sintered Pr-Fe-B (Ref. 14) and $Pr_2Fe_{14}B/\alpha$-Fe (Ref. 15) composite magnets was studied systematically and a nucleation mechanism was proposed to be a leading mechanism in determining the magnetization reversal processes. It is interesting to test whether the coercivity mechanism of the anisotropic Pr-Fe-B thin films is different from that of the sintered ones.

On the other hand, the deposition rate in sputtering is one of the important parameters that affects the microstructure and the magnetic properties of the thin films. Cadieu *et al.* found that films sputtered at a deposition rate lower than 0.18 nm/s exhibited a perpendicular anisotropy, while those deposited at higher deposition rates showed in the planar anisotropy.[16] However, Piramanayagam *et al.* reported that the perpendicular anisotropy was not destroyed even with a higher deposition rate of 0.5 nm/s and the coercivity of films was almost independent of the deposition rate.[17] In our recent work, it was found that the coercivity of the Nd-Fe-B films, crystallized directly on a heated substrate, depended sensitively on the deposition rate.[18] It is also interesting to detect whether the deposition rate can affect the magnetic properties of the Pr-Fe-B thin films which are not crystallized directly on the heated substrate, i.e., prepared by depositing the films at a low substrate temperature and then annealing subsequently at high temperatures.

The aim of this work is to grow the Pr-Fe-B thin films with perpendicular anisotropic texture, to investigate the effect of the deposition rate on the microstructure and the magnetic properties, and to find out the controlling coercivity mechanism of the films. Magnetization reversal behavior can be investigated by various methods, such as initial magnetization curve, minor hysteresis loop, remanence curve,[19–21] micromagnetic model,[22–25] Gaunt model,[26] and so on.

As is known, for $Nd_2Fe_{14}B$, a spin reorientation occurs below 135 K because the magnetocrystalline anisotropy constant K_1 changes sign, while the higher-order magnetocrystalline anisotropy constants K_2 and K_3 also play important roles on its magnetization processes at low temperatures. It was reported, for the Nd-Fe-B magnets, that the expression of the nucleation field in the micromagnetic model should be different in different temperature ranges.[27,28] It seemed rather difficulty to use the same model to describe the temperature dependence of the coercivity of sintered Nd-Fe-B permanent magnets over the whole magnetically ordered temperature range.[28] However, no spin reorientation takes place even

down to 4.2 K for $Pr_2Fe_{14}B$ since the sign of K_1 is always positive, and the magnetocrystalline anisotropy constant $K_1 > 4K_2$ over the whole magnetically ordered temperature range, which guarantees the successful application of the micromagnetic model in the low temperatures.[14,15]

In the present study, the initial magnetization curve, minor hysteresis loop, and remanence curve are first studied to preliminarily distinguish the nucleation model from the domain wall pinning model. Furthermore, with the help of the temperature dependence of coercivity, the micromagnetic model is applied to confirm that the nucleation of reverse magnetization appearing at the grain surface where the magnetic anisotropy is reduced dominates in the temperature range from 5 to 300 K, and to understand whether the grains in the films are strongly magnetically coupled or isolated.

II. EXPERIMENTAL DETAILS

The growth of the thin films was carried out in a high vacuum chamber equipped with multisputtering guns. The base pressure of the chamber was better than 1.5×10^{-5} Pa and the Ar gas pressure was kept at 0.7 Pa during sputtering. A target with a nominal composition of $Pr_{14}Fe_{80}B_6$ and a commercial Mo target of 99.9% purity were used. The deposition rate calibration of the films was measured by weighing. The Pr-Fe-B target was presputtered at least for 30 min to eliminate the oxide layer on the target surface, before deposition of the thin films. All the thin films were prepared with the dc sputtering method on Si (100) substrate heated up to 773 K. Mo buffer and cover layers were deposited in order to protect the Pr-Fe-B layer from oxidation. The deposition rates of the Pr-Fe-B layer were controlled by the target power and the thickness of the Pr-Fe-B layer was fixed to be at 400 nm. The thicknesses of the buffer and cover layer were fixed at 50 nm. After deposition, the films were annealed at 873 K for 30 min in the vacuum better than 2.5×10^{-5} Pa.

The crystalline structure was conducted by x-ray diffraction (XRD) with Cu $K\alpha$ radiation. Magnetic properties were measured with the external magnetic field either perpendicular or parallel to the film plane, using a Quantum Design MPMS-7S superconducting quantum interference device (SQUID) from 5 to 300 K. The room temperature is 295 K in this paper. Atomic force microscopic (AFM) and magnetic force microscopic (MFM) measurements were performed with a scanning probe microscope (Digital Instruments Nanoscope IV) to study the surface morphology and the magnetic domain structure.

III. RESULTS AND DISCUSSION

A. Structure and magnetic properties

Figure 1 shows XRD patterns of Pr-Fe-B thin films before and after annealing, which are deposited with a deposition rate of 0.6 nm/s. For the as-sputtered thin film with substrate temperature $T_s = 773$ K, two primary peaks, Mo (110) ($2\theta \approx 40.6°$) and α-Fe (100) ($2\theta \approx 44.6°$), are observed in Fig. 1(a). No peak, corresponding to the tetragonal $Pr_2Fe_{14}B$ phase, is found because the substrate temperature is below

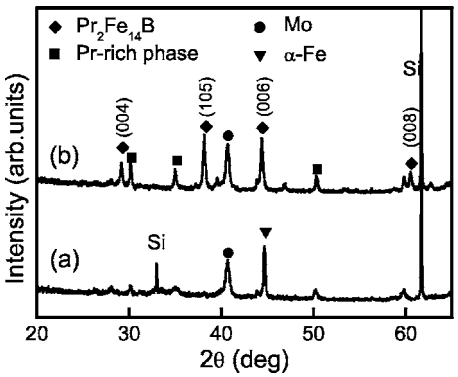

FIG. 1. XRD patterns of Pr-Fe-B thin films before and after annealing with deposition rate 0.6 nm/s: (a) deposited at 773 K and (b) annealed at 873 K for 30 min.

the crystallization temperature of the $Pr_2Fe_{14}B$ phase. After annealing at 873 K for 30 min, the tetragonal $Pr_2Fe_{14}B$ phase appears with obvious c-axis texture in the thin film, as revealed by the strongest XRD peaks for $Pr_2Fe_{14}B$ (006) and (105) lattice plane. In the annealed film, a small amount of Pr-rich phase coexists with the $Pr_2Fe_{14}B$ phase.

Figure 2 represents the hysteresis loops at room temperature of the as-sputtered Pr-Fe-B thin film with the deposition rate of 0.6 nm/s [denoted as a high deposition rate (HR)] and 0.5 nm/s [denoted as a low deposition rate (LR)], measured with the magnetic field parallel to the film plane. The hysteresis loops are of the typical character of soft-magnetic materials because the hard-magnetic $Pr_2Fe_{14}B$ phase is not formed for $T_s = 773$ K, in agreement with the results of the XRD patterns shown in Fig. 1(a). The weak perpendicular magnetic anisotropy (K_A) in the as-sputtered films is estimated by $K_A = M_H H_S/2$, where M_H is the saturation magnetization at an applied field H_S where the hysteresis curves start to saturate.[29,30] The K_A value is estimated to be 0.248 J/cm^3 for the LR thin film and 0.392 J/cm^3 for the HR thin film. The weak perpendicular anisotropy existing in the as-sputtered film is a potential origin of forming a good crystalline texture in the crystallized films and enhancing magnetic properties measured along the direction perpendicular to the film plane. Because the K_A value of the HR thin film is greater than that of the LR thin film, it may be expected that the magnetic properties of the as-annealed HR

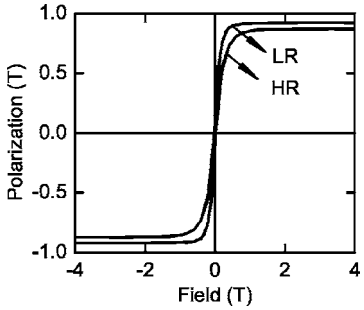

FIG. 2. Hysteresis loops at room temperature of Pr-Fe-B thin film deposited at 773 K, with deposition rates 0.6 nm/s (HR) and 0.5 nm/s (LR). The loops are measured with the magnetic field parallel to the film planes.

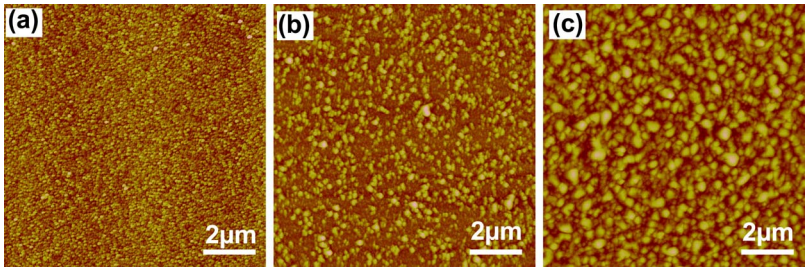

FIG. 3. (Color online) AFM images of as-sputtered Pr-Fe-B thin films with different deposition rates: (a) 0.5 nm/s, (b) 0.7 nm/s, and (c) 0.8 nm/s.

thin film are better than those of the as-annealed LR film.[27]

The microstructure depends on the deposition rate of the as-sputtered Pr-Fe-B thin films, as illustrated in Fig. 3. For lower deposition rate (0.5 nm/s), the film shows homogeneous morphology with the grain size about 100 nm. When the deposition rate increases to 0.7 nm/s, the greater part of the film surface is covered by the grains with a size around 150 nm. When the film is prepared with a higher deposition rate, 0.8 nm/s, the densely packed grains dominate the morphology. The size of these grains ranges from 200 to 400 nm. Generally, the increase of the deposition rate results in more high-energy particles, which equalizes to increase the substrate temperature, so that the grains size increases with increasing the deposition rate.

Figure 4 represents the hysteresis loops at room temperature of the annealed Pr-Fe-B thin films with various deposition rates. After annealing at 873 K for 30 min, the hard-magnetic $Pr_2Fe_{14}B$ phase forms, accompanying an increase of the coercivity. For the same film, an obvious difference is observed for the magnetization recorded with the magnetic fields perpendicular and parallel to the film plane. For both films, the remanent magnetization measured with the applied field perpendicular to the film plane is higher than that with the applied field parallel to the film plane. It indicates the existence of *c*-axis texture perpendicular to the plane of the films, which is consistent with the XRD results shown in Fig. 1(b). The magnetic properties of the Pr-Fe-B thin films, revealed by these hysteresis loops, are sensitive to the deposition rate. For the hysteresis loops measured with the field perpendicular to the film planes, the coercivity $\mu_0 H_{c\perp}$ is 1.45 T and the maximum energy product $(BH)_{max\perp}$ is 193.6 kJ/m^3 (without correcting by demagnetization factor, the same for other data in this work) for the annealed HR Pr-Fe-B thin film, while the coercivity $\mu_0 H_{c\perp}$ decreases to 0.51 T and the maximum energy product $(BH)_{max\perp}$ is 28.3 kJ/m^3 for the as-annealed LR Pr-Fe-B thin film.

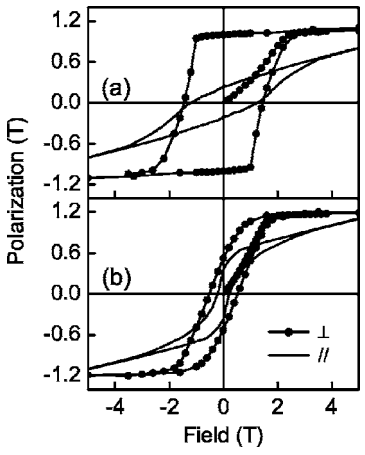

FIG. 4. Hysteresis loops at room temperature of Pr-Fe-B thin film annealed at 873 K for 30 min with different deposition rates: (a) 0.6 nm/s and (b) 0.5 nm/s. The solid lines with/without solid circles represent the loops measured with the magnetic fields perpendicular (⊥)/parallel (||) to the film plane. No demagnetization correction has been carried out for all the measurements.

The deposition rate dependence of the remanences $Mr_\perp$ at room temperature for all the annealed Pr-Fe-B thin films are shown in Fig. 5(a). The ratio of $Mr_\perp/Mr_\parallel$ which can be employed to evaluate qualitatively the degree of texture, is given in Fig. 5(b). It is observed that the ratio of $Mr_\perp/Mr_\parallel$ reaches the maximum when DR=0.6 nm/s, which indicates that more gains with magnetization perpendicular to the film plane are developed after annealing. It may be the reason why the remanence $Mr_\perp$ is highest for DR=0.6 nm/s. However, it is understood that it is very hard to give a quantitative analysis of the degree of texture from the ratio of $Mr_\perp/Mr_\parallel$ because of the lack of a quantitative relationship between them.

Figure 6 shows the deposition rate dependence of the room-temperature coercivities, measured with the field either perpendicular ($\mu_0 H_{c\perp}$) or parallel ($\mu_0 H_{c\parallel}$) to the film plane for the Pr-Fe-B thin films annealed at 873 K for 30 min. It is observed that the coercivity $\mu_0 H_{c\perp}$ is higher than the coercivity $\mu_0 H_{c\parallel}$ for all the thin films. The coercivity $\mu_0 H_{c\perp}$ first increases slowly, then rises abruptly at a certain deposition rate (0.5 nm/s), reaches a maximum at about 1.45 T

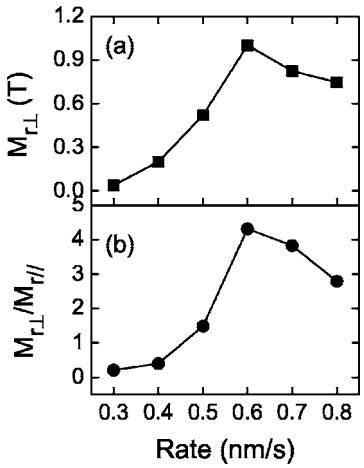

FIG. 5. Deposition rate dependence of (a) the room temperature remanence $Mr_\perp$ and (b) the ratio of $Mr_\perp/Mr_\parallel$ for annealed Pr-Fe-B thin films.

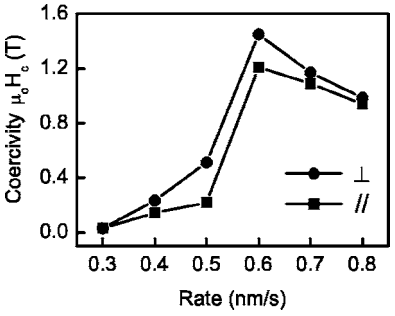

FIG. 6. Deposition rate dependence of the room temperature coercivity of as-annealed Pr-Fe-B thin films.

(0.6 nm/s), and finally decreases with increasing the deposition rate. It is different from the report of Piramanayagam *et al.*[17] that the coercivity was almost independent of the deposition rate. The case in Pr-Fe-B thin films is similar to the tendency observed in Nd-Fe-B thin films.[18] In our recent work, it was found that the atomic ratio of Nd to Fe increased with increasing the deposition rate.[18] With increasing the deposition rate, the atomic ratio of Pr to Fe in the Pr-Fe-B films increases, which results in the appearance of a Pr-rich phase in the Pr-Fe-B thin films. The Pr-rich phase, which usually accounts for the high coercivity, has been observed in the XRD patterns of the thin films prepared with the high deposition rate. So the coercivity increases with increasing the deposition rate firstly. However, excessively increasing the deposition rate brings about two effects: one is more bombardment of high-energy particles emitted from the target, which leads to the films tending to grow isotropiclike, another is the excessive growth of the grains as shown in Fig. 3. The former leads to the decrease of the remanence $Mr_{\perp}$ and the ratio of $Mr_{\perp}/Mr_{\parallel}$. The latter results in the decrease of coercivity. The change of the film composition can also explain why the saturation magnetization of the LR film is higher than that of the HR film as shown in Fig. 2. This is because the ratio of Fe to Pr for as-sputtered LR thin film is higher than that of as-sputtered HR thin film.

B. Coercivity mechanism

The initial magnetization curves at room temperature for as-annealed HR and LR thin films are shown in Fig. 4, respectively. Though the magnetization increases linearly with external magnetic field, it is a little difficult to determine the type of the coercivity mechanism for the films. It seems that both nucleation-type and pinning-type mechanisms coexists in magnetization reversal processes for both the films. In order to understand which kind of coercivity mechanism dominates the magnetization reversal processes, the minor loops and remanence curves are investigated for as-annealed HR and LR thin films.

Figure 7 shows the field dependence of the coercivity $\mu_0 H_{c\perp}$ for as-annealed HR and LR thin films at room temperature. The coercivities increase linearly with magnetization field and then saturate, which suggests that the nucleation of magnetization reversal is dominant in both the as-annealed HR and LR thin films.[31,32]

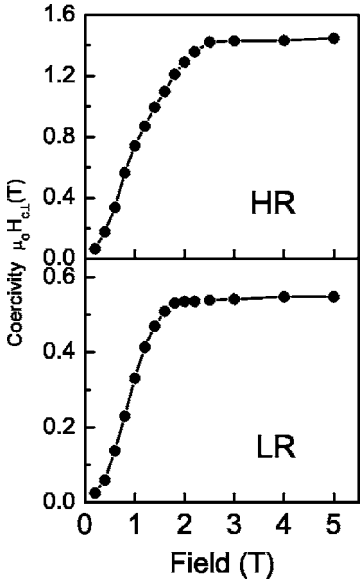

FIG. 7. External magnetic field dependence of the room-temperature coercivity of as-annealed HR and LR Pr-Fe-B thin films.

The remanence curves have been applied to study the coercivity mechanism by many researchers.[19,20] The remanence data are fitted to the remanence curve relationship[21]

$$M_D(H) = M_R(\infty) - 2M_R(H), \tag{1}$$

where $M_R(H)$ is the initial remanence resulting from the application of a positive field H, $M_R(\infty)$ is the saturation remanence, and $M_D(H)$ is the demagnetization remanence obtained with a reverse field of magnitude H. Equation (1) should be obeyed for noninteracting single domain particles and for uniform domain wall pinning where the domain walls encounter the same type of pins in the initial magnetization and demagnetization state. The values of $M_R(H)$ and $M_D(H)$ have been measured for as-annealed HR thin film with a field perpendicular to the film plane at room temperature and $M_D(H)/M_R(\infty)$ against $M_R(H)/M_R(\infty)$ is shown in Fig. 8. The data, in consideration of a demagnetization factor $N=0.3$, is also given in Fig. 8 (The upper limit of N is about 0.3 for the annealed HR thin film. For $N>0.3$, the hysteresis loop of the annealed HR thin film will be S-shaped and meaningless.) If Eq. (1) is obeyed, the data points should fall on the straight line joining $M_R(H)/M_R(\infty)=0$, $M_D(H)/M_R(\infty)=1$ to $M_R(H)/M_R(\infty)=1$, $M_D(H)/M_R(\infty)=-1$, as shown in Fig. 8. However, the data (either with or without demagnetization correction) deviates from the ideal line obviously, which suggests that the pinning type mechanism is indeed not dominant in the magnetization reversal processes of as-annealed HR thin film.

In order to study the coercivity mechanism in more detail, the temperature dependence of the coercivity is investigated with the micromagnetic model.[22–25] According to the micromagnetic model,[22–25] the coercivity H_c can be generally expressed as $(K_1>4K_2)$:

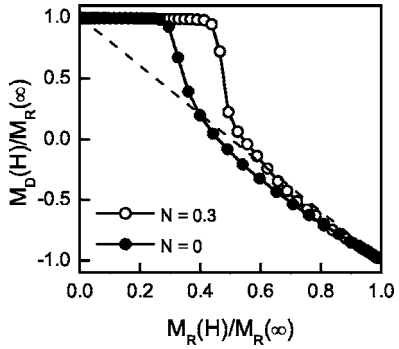

FIG. 8. $M_D(H)/M_R(\infty)$ vs $M_R(H)/M_R(\infty)$ of as-annealed HR Pr-Fe-B thin film. The solid lines with solid and open circles, respectively, correspond to the data with demagnetization factor $N=0$ and 0.3. The dashed straight line describing Eq. (1) is for noninteracting single domain particles and for uniform domain wall pinning.

$$H_c = \alpha_K a_\varphi \frac{2K_1}{\mu_0 M_s} - N_{eff} M_s \tag{2}$$

where H_c, K_1, N_{eff}, and M_s are the coercivity, the first-order anisotropy constant, the effective local demagnetization factor, and the saturation magnetization, respectively. α_K and α_φ are microstructural coefficients. The coefficient α_φ describes the reduction of the coercivity due to misaligned grains, while the coefficient α_K represents the reduction of the coercivity due to the inhomogeneous nucleation regions, e.g., near the grain surface. If the microstructural parameters α_K and N_{eff} are constants and temperature independent, one can determine the parameters α_K and N_{eff} by plotting H_c/M_s vs $2K_1/\mu_0 M_s^2$. This plot should yield a line with the slope α_K and its intersection N_{eff} with the ordinate.

In the case of nucleation controlled magnets, the microstructural parameters α_φ and α_K for an isolated grain have been shown theoretically:[24,25]

$$a_\varphi = \frac{1}{\cos\varphi}\frac{1}{(1+\tan^{2/3}\varphi)^{3/2}}\left(1+\frac{2K_2}{K_1}\frac{\tan^{2/3}\varphi}{1+\tan^{2/3}\varphi}\right), \tag{3}$$

where φ is the angle between the applied field and the negative c axis, and

$$\alpha_K = 1 - \frac{1}{4\pi^2}\frac{\delta_B^2}{r_0^2}\left[-1+\left(1+\frac{4\Delta K r_0^2}{A}\right)^{1/2}\right]^2, \tag{4}$$

where δ_B, ΔK, A, and r_0 are the domain-wall width, a reduction of the anisotropy constant K_1 by ΔK, the exchange constant, and the half-width of the planar perturbed inhomogeneous region of width $2r_0$, respectively.

Both as-annealed HR and LR Pr-Fe-B thin films have the same hard-magnetic $Pr_2Fe_{14}B$ phase as the matrix phase. Therefore, for both films, the intrinsic magnetic properties, i.e., the anisotropy constants, the spontaneous magnetization, etc., are the same as those of the $Pr_2Fe_{14}B$ phase. The temperature dependence of the anisotropy constants K_1 and K_2 of $Pr_2Fe_{14}B$ is taken from Ref. 14, and the temperature dependence of the saturation magnetization M_s of $Pr_2Fe_{14}B$ is taken from Ref. 33. Figure 9 shows the temperature dependence of the coercivity $\mu_0 H_{c\perp}$ of the as-annealed HR and LR films. The coercivity increases monotonically with decreasing temperature for both the thin films. The coercivity $\mu_0 H_{c\perp}$ of as-annealed HR thin film is higher than that of as-annealed LR thin film in the temperature range from 5 to 300 K.

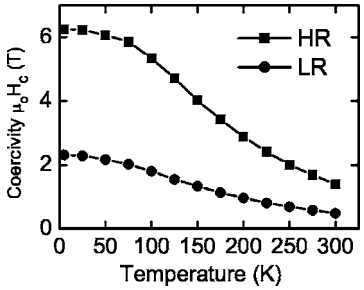

FIG. 9. Temperature dependence of the coercivity $\mu_0 H_{c\perp}$ of as-annealed HR and LR Pr-Fe-B thin films.

The analysis based on the micromagnetic model for the nucleation mechanism is performed in the following steps.

(1) In order to test whether the magnetization reversal process in the anisotropic Pr-Fe-B thin films is controlled by a uniform rotation of the magnetic moments, H_c/M_s vs $2K_1/\mu_0 M_s^2$ is plotted in Fig. 10. It can be seen that a linear relationship exists in the temperature range from 150 to 300 K for both HR and LR thin films. If the magnetic moments rotate uniformly and coherently in the Pr-Fe-B thin films, the slopes of these lines should be 1. In fact, the fitted result is 0.27 for the HR film and 0.09 for the LR film, respectively. Therefore it is concluded that the actual magnetization reversal processes in Pr-Fe-B thin films are not realized by uniform rotations of the magnetic moments.

(2) When the grains in the films are strongly magnetically coupled, a reversion of a misaligned grain induces the reversion of the magnetization in the neighboring grains. So the coercivity depends only on these grains that have the minimum nucleation field.[14,25,34] In this case, $\alpha_\varphi = \alpha_\varphi^{\min}$, where $\alpha_\varphi^{\min}$ is the minimum of Eq. (3). According to Eq. (3), the coefficient α_φ can be calculated for a given temperature.

Figure 11 gives the calculated results for Pr-Fe-B thin films at 5, 100, and 300 K and the minima $\alpha_\varphi^{\min}$ for different

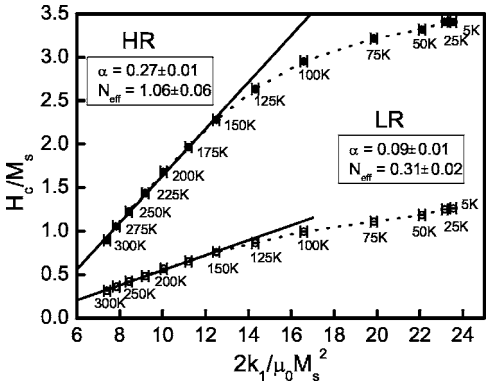

FIG. 10. Plot of H_c/M_s vs $2K_1/\mu_0 M_s^2$ for as-annealed HR and LR Pr-Fe-B thin films to test the nucleation model under the assumption that magnetization reverses coherently.

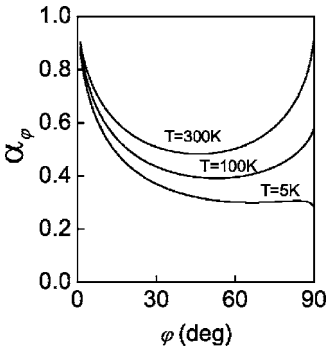

FIG. 11. Angular dependence of α_φ calculated for $Pr_2Fe_{14}B$ at $T=300$, 100, and 5 K.

temperatures can be taken from these curves. The value of $\alpha_\varphi^{\min}$ is about 0.3–0.5 in the temperature range from 5 to 300 K, which decreases with decreasing temperature. It is also shown that the angle ($\varphi_{\min}$), corresponding to $\alpha_\varphi^{\min}$ depends on temperature, particularly at low temperatures (<200 K), where the absolute value of K_2/K_1 is large, e.g., the angle $\varphi_{\min}=46°$, 53°, and 66° at 300, 100, and 5 K, respectively. However, with decreasing temperature, the tendencies of $\alpha_\varphi^{\min}$ and $\varphi_{\min}$ for the Nd-Fe-B magnet are opposite those of the Pr-Fe-B magnet.[27] It was reported that with decreasing temperature, the value of $\alpha_\varphi^{\min}$ increased to 1 at about $T=170$ K and kept with 1 at $T<170$ K for Nd-Fe-B magnets.[27] The different behaviors between $\alpha_\varphi^{\min}$ (or $\varphi_{\min}$) of $Nd_2Fe_{14}B$ and $Pr_2Fe_{14}B$ are mainly due to the fact that these two compounds have different signs of K_2/K_1 ratio (positive for $Nd_2Fe_{14}B$ at $T>135$ K, while negative for $Pr_2Fe_{14}B$). The different values and signs of K_2/K_1 finally result in different behaviors between $\alpha_\varphi^{\min}$ of $Nd_2Fe_{14}B$ and $Pr_2Fe_{14}B$ through Eq. (3).

Figure 12 shows the plot of H_c/M_s vs $2\alpha_\varphi^{\min}K_1/\mu_0M_s^2$ for as-annealed HR and LR thin films. The purpose of this step is to test whether the magnetization reverse processes of HR or LR thin films are controlled by the nucleation mechanism with the grains strongly magnetically coupled. It is evident that a nearly perfect linear relationship exists over the whole investigated temperature, which indicates that the coercivity of as-annealed HR and LR Pr-Fe-B films is in agreement

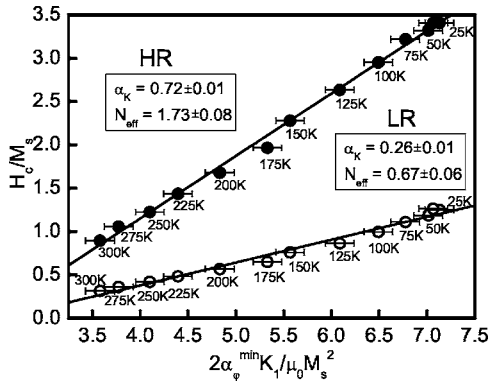

FIG. 12. Plot of H_c/M_s vs $2\alpha_\varphi^{\min}K_1/\mu_0M_s^2$ for as-annealed HR and LR Pr-Fe-B thin films to test the nucleation model under the assumption that grains are strongly magnetically coupled.

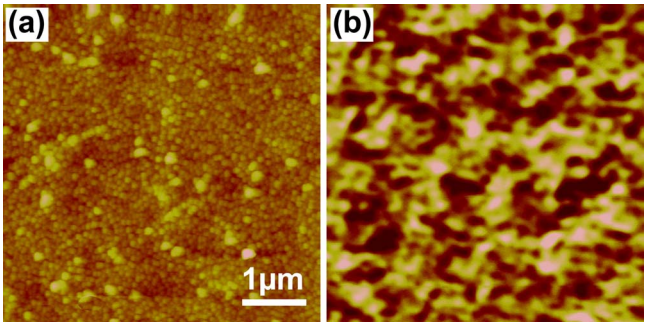

FIG. 13. (Color online) AFM (a) and MFM (b) images for as-annealed HR Pr-Fe-B thin film.

with Eq. (1) under the assumption $\alpha_\varphi=\alpha_\varphi^{\min}$. So we can judge the type of the coercivity mechanism through the micromagnetic parameters α_K by fitting the data. By using a least-squares-fitting program, the micromagnetic parameters α_K and N_{eff} are determined. It is interesting to observe that N_{eff} of HR thin film ($N=1.73$) is higher than that of LR thin film ($N_{eff}=0.67$). As shown in Fig. 9, the coercivity of HR thin film is always greater than that of LR thin film. It is different from the case reported in sintered Pr-Fe-B magnets,[14] where the magnet with higher coercivity has a smaller N_{eff}. The reason is that according to the micromagnetic model, the coercivity is determined by the two terms in Eq. (2): not only by the effective local demagnetization factor N_{eff} in the second term, but also by other factors in the first term.

According to the micromagnetic model,[25] values of $\alpha_K>0.3$ are only compatible with the nucleation mechanism, whereas values of $\alpha_K<0.3$ may include both pinning as well as nucleation mechanisms. As shown in Fig. 12, the coefficients α_K of HR and LR thin films are 0.72 and 0.26, respectively. So it is confirmed that the nucleation mechanism is the leading mechanism for the as-annealed HR thin film. Though the value of α_K is 0.26 for LR thin film, a little smaller than 0.3, the magnetization reverse mechanism for this film should be also the nucleation mechanism, considering the initial magnetization curve and the field dependence of the coercivity shown above. Inputting α_K into Eq. (4) (and assuming $\Delta K=0.9K_1$), we obtain $r_0/\delta_B=0.27$ for the as-annealed HR film, and $r_0/\delta_B=1.71$ for the as-annealed LR film. It indicates that the inhomogeneous thickness r_0 in as-annealed LR thin film is much greater than that in as-annealed HR thin film when δ_B is assumed to be the same for both the films at the same temperature.

For the above analysis, it is evident that the nucleation model gives a satisfying description of the coercivity of the anisotropic Pr-Fe-B thin film and it can therefore be concluded that the magnetization reversal processes of these films is determined by the nucleation mechanism with the grains strongly magnetically coupled. It is similar to the coercivity mechanism reported in the sintered Pr-Fe-B magnets.[14]

Figure 13 shows the AFM and MFM images of as-annealed HR thin film. The thin film shows a rather inhomogeneous morphology with small grains about 100 nm in the background and some larger grains with the size around 150–200 nm on the top of the smaller grains. The MFM

image shows a bright-dark contrast with an irregular shape. The domain sizes are about several hundred nanometers, much larger than that of the grains, which indicates that several grains are coupled magnetically in one domain. It is in agreement with the discussion of the coercivity mechanism.

IV. CONCLUSIONS

The perpendicular anisotropic Pr-Fe-B thin films have been prepared by depositing the films at a low substrate temperature followed the annealing. The effects of the deposition rate on the microstructure and magnetic properties have been studied. The existence of a weak anisotropy in the as-deposited films results in the perpendicular anisotropy of the crystallized films. The magnetic properties of the anisotropic Pr-Fe-B thin films depend sensitively on the deposition rate. The coercivity as high as 1.45 T is obtained and the best value of the maximum energy product is 193.6 kJ/m^3 for the film with the deposition rate of 0.6 nm/s. The coercivity mechanisms of the anisotropic Pr-Fe-B thin films have been investigated systematically. The studies based on the micromagnetic model show that the magnetization reversal process of the anisotropic Pr-Fe-B thin films is determined by a nucleation process of reversed domains, and the grains in the thin films are strongly magnetically coupled. The magnetization reversal processes in Pr-Fe-B thin films are not realized by uniform rotations of the magnetic moments.

ACKNOWLEDGMENTS

This work has been supported by the National Nature Science Foundation of China under Project Nos. 50331030 and 50371085 and the National 863 Project under Grant No. 2002AA302603.

[1] S. Yamashita, J. Yamasaki, M. Ikeda, and N. Iwabuchi, J. Appl. Phys. **70**, 6627 (1991).
[2] H. Lemke, T. Lang, T. Göddenhenrich, and C. Heiden, J. Magn. Magn. Mater. **148**, 426 (1995).
[3] J. F. Zasadzinski, C. U. Segre, and E. D. Rippert, J. Appl. Phys. **61**, 4278 (1987).
[4] V. Neu, S. Melcher, U. Hannemann, S. Fähler, and L. Schultz, Phys. Rev. B **70**, 144418 (2004).
[5] F. J. Cadieu, T. D. Cheung, and L. Wickramasekara, J. Magn. Magn. Mater. **54-57**, 535 (1986).
[6] D. J. Keavney, E. E. Fullerton, J. E. Pearson, and S. D. Bader, IEEE Trans. Magn. **32**, 4440 (1996).
[7] A. J. M. Geurtsen, J. C. S. Kools, L. de. Wit, and J. C. Lodder, Appl. Surf. Sci. **96-98**, 887 (1996).
[8] K. D. Durst and H. Kronmüller, J. Magn. Magn. Mater. **68**, 63 (1987).
[9] A. Melsheimer and H. Kronmüller, Physica B **299**, 251 (2001).
[10] J. L. Tsai and T. S. Chin, J. Magn. Magn. Mater. **196-197**, 728 (1999).
[11] A. Kruusing, Int. Mater. Rev. **44**, 121 (1999).
[12] K. D. Aylesworth, D. J. Sellmyer, and G. C. Hadjipanayis, J. Magn. Magn. Mater. **98**, 65 (1991).
[13] K. D. Aylesworth, D. J. Sellmyer, and G. C. Hadjipanayis, J. Appl. Phys. **67**, 5725 (1990).
[14] X. C. Kou, H. Kronmüller, D. Givord, and M. F. Rossignol, Phys. Rev. B **50**, 3849 (1994).
[15] D. Goll, M. Seeger, and H. Kronmüller, J. Magn. Magn. Mater. **185**, 49 (1998).
[16] F. J. Cadieu, T. D. Cheung, L. Wickramasekara, and N. Kamprath, IEEE Trans. Magn. **22**, 752 (1986).
[17] S. N. Piramanayagam, M. Matsumoto, and A. Morisako, J. Appl. Phys. **85**, 5898 (1999).
[18] S. L. Chen, W. Liu, and Z. D. Zhang, J. Magn. Magn. Mater. (to be published).
[19] J. Ding, R. Street, and P. G. McCormick, J. Magn. Magn. Mater. **115**, 211 (1992).
[20] G. C. Hadjipanayis and A. Kim, J. Appl. Phys. **63**, 3310 (1988).
[21] E. P. Wohlfarth, J. Appl. Phys. **29**, 595 (1958).
[22] H. Kronmüller, Phys. Status Solidi B **130**, 197 (1985).
[23] G. Herzer, W. Fernengel, and E. Adler, J. Magn. Magn. Mater. **58**, 48 (1986).
[24] H. Kronmüller, K. D. Durst, and G. Martinek, J. Magn. Magn. Mater. **69**, 149 (1987).
[25] H. Kronmüller, K. D. Durst, and M. Sagawa, J. Magn. Magn. Mater. **74**, 291 (1988).
[26] J. F. Liu and H. L. Luo, J. Magn. Magn. Mater. **86**, 153 (1990).
[27] X. C. Kou and H. Kronmüller, J. Phys.: Condens. Matter **6**, 6691 (1994).
[28] J. Hu, X. C. Kou, and H. Kronmüller, Phys. Status Solidi A **138**, K41 (1993).
[29] L. K. E. B. Serrona, A. Sugimura, N. Adachi, T. Okuda, H. Ohsato, I. Sakamoto, A. Nakanishi, M. Motokawa, D. H. Ping, and K. Hono, Appl. Phys. Lett. **82**, 1751 (2003).
[30] B. X. Gu, H. Homburg, S. Methfessel, and H. R. Zhai, Phys. Status Solidi A **120**, 159 (1990).
[31] J. B. Yang, O. Gutfleisch, A. Handstein, D. Eckert, and K. H. Müller, Appl. Phys. Lett. **76**, 3627 (2000).
[32] H. Okumura, F. Zhang, and G. C. Hadjipanayism, J. Appl. Phys. **91**, 6147 (2002).
[33] S. Hirosawa, Y. Matsuura, H. Yamamoto, S. Fujimura, M. Sagawa, and H. Yamauchi, J. Appl. Phys. **59**, 873 (1986).
[34] X. C. Kou, W. J. Qiang, H. Kronmüller, and L. Schultz, J. Appl. Phys. **74**, 6791 (1993).